Electromagnetic dissociation of ^{32}S at ultrarelativistic energy in nuclear emulsion

G. Singh, K. Sengupta, and P. L. Jain
High Energy Experimental Laboratory, Department of Physics, State University of New York at Buffalo, Buffalo, New York 14260
(Received 16 March 1989)

Electromagnetic dissociation of 200 GeV/nucleon ^{32}S projectiles has been investigated in nuclear emulsion. It constitutes about 15% of the total number of events observed. The production cross section for the electromagnetic process has been found to increase with the projectile charge when compared with that of the ^{16}O beam at the same energy per nucleon.

I. INTRODUCTION

The acceleration of heavy nuclei to ultrarelativistic energies at Brookhaven and CERN has opened new areas of research in particle and nuclear physics. The main objective of the study of nucleus-nucleus collisions at such energies is to observe the signatures of new forms of nuclear matter like the quark-gluon plasma (QGP) at very small values of the impact parameter of collision. However, in collisions involving impact parameters larger than the range of the nuclear force, extremely strong electromagnetic fields are produced for a short period of time. These varying electromagnetic fields have also led to an interesting domain of physics that has not been explored in a systematic way in heavy-ion collisions in the past.

In relativistic heavy-ion collisions, electromagnetic dissociation (ED) of the projectile nucleus is thought to take place via the exchange of a virtual photon between the target nucleus and the projectile.[1,2] According to the classical theory of Weiszacker and Williams,[3] the spectrum of virtual photons as seen by the projectile from a point target nucleus, may be represented by a rapidly varying time-dependent electromagnetic field. The number of photons per unit energy interval, dN/dE_γ, is approximately proportional to $Z_T^2(\ln\gamma/E_\gamma)$, where Z_T is the target charge, γ is the Lorentz factor of the projectile in the laboratory frame, and E_γ is the photon energy. The virtual photon spectrum has an adiabatic cutoff at an energy $E_{\gamma_{\max}} \simeq \gamma\hbar c/b_{\min}$, where $b_{\min}=R_P+R_T$, the sum of the projectile and target radii. At Bevalac energies ($\sim$2 GeV/nucleon), $E_{\gamma_{\max}} \simeq 40$ MeV, while at CERN energies ($\sim$200 GeV/nucleon), $E_{\gamma_{\max}} \simeq 4$ GeV. Electromagnetic interaction of the projectile with a photon below 40 MeV usually produces giant multipole resonances, which cause a target nucleus to deexcite through the emission of evaporation fragments. On the other hand, photons with energy $E_{\gamma_{\max}} \simeq 4$ GeV can interact with a single nucleon, exciting a Δ (1232) resonance that decays into a nucleon and a pion, either of which can initiate a two-step process of intranuclear cascade accompanied by evaporation tracks similar to those seen in proton-nucleus interactions.

So far, only a few experiments have been performed to deal with ED of different projectiles at ultrarelativistic energies.[4–7] Some of this work was also done with heavy primaries in cosmic rays.[8] The aim of the present experiment is to study the electromagnetic dissociation of the ^{32}S projectile at the highest available energy (200 GeV/nucleon) from the CERN Super Proton Synchrotron (SPS) in nuclear emulsions. An attempt has been made to distinguish, in an independent way, between the reaction mechanism involved in ED and nuclear interactions by studying the multiplicity distribution of the projectile alpha fragments emerging from ED's under the perspective of a Koba-Nielsen-Olesen (KNO) distribution. It is well known that the emulsion detector covers a 4π geometry and has a very high spatial resolution. The latter feature is very helpful in identifying and measuring the angles of individual fragments of the projectile (PF's) which are emitted during the breakup in an ED event.

The paper is arranged as follows. In Sec. II we describe the experimental procedure. This includes scanning and selection of events, charge determination of PF's, event classification, and measurement of the polar angles. Section III is devoted to the discussion of our experimental results which includes the charge spectrum of the PF's and the measurements of the total and partial cross sections. The transverse momentum distribution of protons in the ^{31}Pp mode is discussed here, followed by a discussion of the multiplicity distribution of alpha fragments emitted in ED's. Finally, Sec. IV contains the concluding remarks.

II. EXPERIMENTAL PROCEDURE

A. Scanning and selection of events

In the present experiment, we have employed a stack consisting of 36 Ilford G5 nuclear emulsions of dimensions $18\times7.5\times0.06$ cm^3, exposed horizontally to the 200 GeV/nucleon ^{32}S ions at the CERN SPS. The beam flux density was 1×10^3 ions/cm^2. In order to obtain an unbiased sample of events, an along-the-track scanning technique was adopted. The pellicles were scanned under $100\times$ magnification using oil immersion objectives in digitized microscopes. The beam tracks were picked up at a distance of 4 mm from the edge of the pellicle and were carefully followed until they either interacted with nuclei of the emulsion or escaped from the pellice. If an interaction occurred the following characteristic features were recorded: N_b, the number of black tracks (mostly protons of kinetic energies $E<40$ MeV); N_g, the number of grey tracks (recoil protons in the kinetic energy range

$40 < E < 400$ MeV); n_s, the number of minimum ionizing shower tracks; N_f, the number of projectile fragments (PF's) of charge $Z \geq 2$ (see later).

B. Charge determination of PF's

The charges of all the PF's ($Z \geq 2$) were determined by measurement of grain density and gap density and by counting of δ rays[9] in a fixed track length. Specifically, the method of grain and gap counting was applied to discriminate between charges up to $Z \approx 8$ and the measurements were made over 3–4 mm of track length. On the other hand, for PF's in the charge range $8 < Z < 16$, we counted δ rays in 2 cm of track length. The charge resolution was estimated to be ± 1 charge unit for $Z \geq 9$.[9]

C. Event classification

Each event was qualitatively classified into two principal categories depending upon visual characteristics.

(1) Nuclear events: Nuclear events may be central or peripheral.

Central events: Events which exhibit *no* PF's of charge $Z \geq 2$ in the forward cone; such events are thought to be produced by violent destruction of the projectile and target nuclei at small values of the impact parameter (b) of collision.

Peripheral events: Events with PF's of charge $Z \geq 2$ emitted in a forward cone. Formed at relatively large values of b, peripheral or grazing collisions are thought to be those in which part of the projectile that overlaps the target nucleus may be sheared off by the impact. The remaining nuclear matter proceeds with near beam velocity as fragments of nuclei of reduced charge and/or mass, alpha particles, and nucleons. (There is no established criterion of separation of central and peripheral events. Some authors use more stringent selection criterion based on the setting of a lower limit on n_s and $N_h = N_b + N_g$ to ensure collisions with a heavy nuclear target in emulsion.)

(2) Electromagnetic events: Events generated by the electromagnetic dissociation of the projectile nucleus are generated in collisions involving impact parameters large enough so that no nuclear interactions occur. Extremely strong electromagnetic fields from the heavy nuclei are produced for a very short time at the projectile; such events typically consist of PF's, which proceed essentially in the direction of the projectile nucleus.

We followed a total track length of 127.38 m, during which 1354 events were observed, giving rise to a total interaction mean free path $\lambda = 9.41 \pm 0.26$ cm. In this analysis it is very important to distinguish peripheral events from electromagnetic dissociations, since the former class of events may, in some cases, exhibit topologies similar to the latter. Confusion may arise in grazing collisions where a few pion tracks are produced in addition to the projectile protons. In order to achieve the necessary distinction, we have used the concept of "fragmentation cone" for the projectile fragments.[10] The fragmentation cone was defined by $\Theta_{\rm PF} \leq \Theta_c = p_f / p_{\rm beam}$, where p_f is the Fermi momentum, estimated to be ≈ 200 MeV/c ($\Theta_c \simeq 1$ mrad at 200 GeV/nucleon). The value of Θ_c was chosen such that the probability of finding the produced shower particles among the projectile fragments (in grazing collisions) in the fragmentation cone is very low.[10] The ED's were then picked up using the criterion that the total charge of the PF's ($Z \geq 1$) inside this cone is 16.[10]

The contribution of the peripheral events in the sample of electromagnetic dissociations (where charged particles are emitted) is effectively removed by the requirement that $n_s \leq 1$. Since the reaction channels $^{32}S(\gamma,2n)^{30}S$, $^{32}S(\gamma,3n)^{29}S$, etc., cannot be observed in nuclear emulsion, a correction was applied to the experimental ED cross section (see Sec. III C). In order to eliminate events produced by elastic collisions, events with a single black or grey track emerging from the undeviated beam track were not considered. To avoid inclusion of fast δ rays and low-energy e^+e^- pairs sitting on the beam tracks, the events with a single shower track were reexamined under high magnification. If the shower track under consideration showed significant effects of Coulomb scattering when followed for at least 3 cm, the event was not included in our sample. After applying the above stringent selection criteria, 197 events were found to be produced by electromagnetic interactions, out of a total of 1354 observed events. In our sample of 197 events, 179 were clean breakups of the projectile, with no pion tracks and no visible excitation of the target (N_b or $N_g = 0$). Five events showed a small amount of target excitation along with projectile fragmentation and with no pion tracks, while five more showed only slight target excitations and no projectile breakup. The remaining eight events showed no target excitation, but projectile fragmentation accompanied by a single pion track.

D. Polar angle measurement

The polar angles (θ) of all tracks were determined from the vector directions of the incident and emitted tracks by measuring the xyz coordinates of at least four points along each track including the vertex. The points on each track were often taken 1 mm apart, depending upon its multiple Coulomb scattering in the detector. These measurements were made under a special (UMW-11 Leitz) microscope, digitized in units of 0.1 μm. The coordinates were then subjected to three-dimensional track reconstruction programs based on the method of least squares to determine the best-fit lines, the vector directions of which gave the projected (ϕ), dip (δ), and polar (θ) angles. The errors in the polar angles (ϵ_θ), caused by multiple Coulomb scattering, were determined from the errors in the dip (ϵ_δ) and projected angle (ϵ_ϕ), separately, by the following method, a comprehensive discussion of which can be found in Ref. 11. The average errors in polar angles were calculated by taking all the instrumental errors due to reading, stage, grain, etc., into account. (ϵ_θ) was then calculated from

$$\epsilon_\theta = \cot\theta[(\tan\phi)^2\epsilon_\phi^2 + (\tan\delta)^2\epsilon_\delta^2] ,$$

where $\epsilon_\phi^2 = (ct/p^2\beta^2) + c_1 t^2$ and $\epsilon_\delta^2 = (ct/p^2\beta^2) + c_2 t^2$.

Here, t is the cell length used, $p\beta$ is the particle energy and c_1, c_2 contain the noise contributions from reading, stage and grain, etc., noises. We found that the errors in the polar angles were small compared to their absolute value. A typical value of (ϵ_θ) is ~ 0.2 mrad for the smallest angles measured.

III. RESULTS

A. The charge spectrum

The charge spectrum of all the PF's ranging from protons to ^{31}P is shown in Fig. 1. The most abundant PF is the one with charge $Z=1$, the next with $Z=2$. The least abundant charges are in the range $3 \leq Z \leq 11$, after which there is a gradual increase in the relative abundances. $Z=15$ is almost 1.5 times as abundant as $Z=14$.

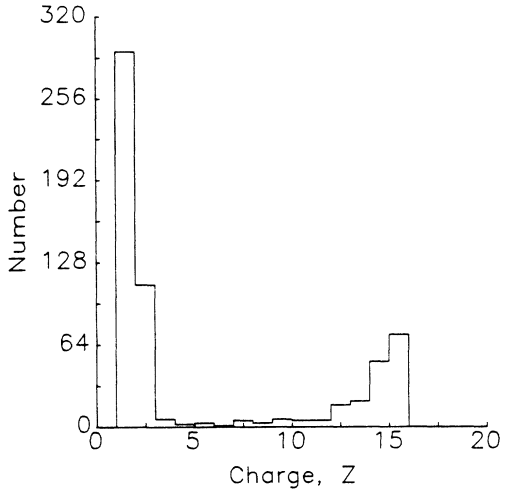

FIG. 1. Charge spectrum of the PF's $1 \leq Z \leq 15$ emitted in ED events.

B. The cross sections, σ_{em}, σ_{nuc}, and σ_{tot}

Table I presents the topologies of ^{32}S interactions of this experiment as compared to the ^{16}O data of Refs. 7 and 12. The number of ED's, as a percentage of the total number of events in the sample, is seen to increase with the projectile energy and mass. The mean free path for the overall ED process, corrected for the undetectable ^{31}Sn, ^{30}S2n, ^{29}S3n, etc., modes, is 0.42 ± 0.02 m, which leads to the experimental ED cross section, $\sigma_{em}=511 \pm 29$ mb. The correction procedure is discussed in further detail in Sec. III C. The theoretical value of this cross section, σ_{em}^{th}, was computed using the method outlined in Refs. 5 and 6. Using the average charge of the emulsion nuclei, $Z_T=21.52$,[13] σ_{em}^{th} was estimated to be 345 mb. The production cross section for nuclear events [calculated from $\sigma=1/\rho\lambda$, where $\rho=7.898\times10^{22}$ atoms/ml (Ref. 13) in emulsions and $\lambda=11.01 \pm 0.32$ cm, the observed mean free path for nuclear interactions (see Table I)], σ_{nuc}, is found to be 1150 ± 34 mb. Finally, the total cross section, $\sigma_{tot}=\sigma_{nuc}+\sigma_{em}$, for ^{32}S-emulsion interactions is 1661 ± 43 mb. In order to compare the experimentally obtained value of σ_{nuc} with a theoretical prediction, we have used the semiempirical expression of σ_{nuc} given by Westfall *et al.*:[14]

$$\sigma_{nuc}^{th}=\pi[r_0(A_P^{1/3}+A_T^{1/3}-b)]^2 , \quad (1)$$

where $r_0=1.35$ fm and $b=0.83$. Since this formula is valid for $A_P \geq 12$ and $A_T \geq 12$, we used $A_T=48.39$ for nuclear emulsion[13] after neglecting the contribution from the ^{1}H targets and obtained $\sigma_{nuc}^{th}=2053$ mb with $A_P=32$. The corresponding experimental values of σ_{nuc}, after excluding the contribution of the ^{1}H targets, is found to be 1940 ± 57 mb, showing that these values are in close agreement.

In Fig. 2, we plot the experimental values of the overall cross section, σ_{em}, for the ED process as a function of the target charge Z_T. Also shown in this figure are the data points of Price, Guoxiao, and Williams[4] and Brechtmann and Heinrich.[6] The following functional form was obtained after a least-squares fitting of the data:

$$\sigma_{em}=cZ_T^d , \quad (2)$$

where $c=0.75 \pm 1.51$ and $d=2.02 \pm 0.12$ with $\chi^2/DF=0.009$. It is interesting to note that $d=2$ is expected for a point target nucleus (see Sec. I), which is obviously not the situation in this experiment.

C. Partial production cross sections in ED's

In Table II, the various partial modes of breakup of the ^{32}S projectile due to ED are given. The most prominent modes of breakup are ^{31}Pp, SiHe, Si2p, AlHep, and MgHe2p in descending order. It should be noted that, in this experiment only the charge of each PF is determined. The mass of the fragment (when quoted in Table II) is speculative and stable isotopes of heavy fragments may as well be produced. Since neutrons cannot be detected in emulsions, the disintegration mode ^{31}Sn, expected to be similar to the ^{31}Pp mode, has escaped detection. Furthermore, the mode ^{30}Ppn cannot be distinguished from the ^{31}Pp mode, and so on. In Table II, we have also included the experimental value of σ_{em} which has been determined

TABLE I. Topologies of ^{32}S interactions as compared to ^{16}O interactions at 200 and 60 GeV/nucleon in nuclear emulsion.

Beam	Energy (GeV/nucleon)	Reference	Track length followed (m)	Total no. of events (p)	No. of nuclear events	No. of ED's (r)	ED as % of all events $(r/p)\times100$
^{32}S	200	This experiment	127.38	1354	1157	197	14.55
^{16}O	200	7	69.12	663	591	72	10.86
^{16}O	60	12	63.53	528	497	31	5.87

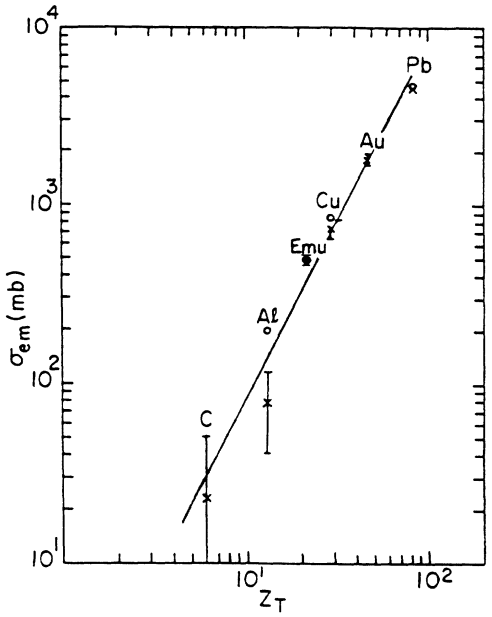

FIG. 2. Overall production cross section, σ_{em}, as a function of the target charge, Z_T. (●) This experiment; (○) Price, Guoxiao, and Williams (Ref. 4); (×) Ref. 6. The solid line drawn in this figure is the fitted function given by Eq. (2) (see text).

on the basis of the assumption that the dissociation modes ^{30}Ppn are detected as ^{31}Pp and the mode ^{31}Sn contributes as ^{31}Pp. Also, the mode ^{30}S2n, is assumed to contribute as ^{30}Si2p, ^{29}S3n as ^{29}Al3p, etc. Furthermore, we have neglected the contribution of ^{1}H nuclei in emulsion, because even at CERN energies, $\sigma_{em}(P=^{32}\text{S}, T=\text{H}) \approx 1$ mb.[5,6] The major contribution to the ED process in the emulsion comes from Ag ($Z=47$) and Br ($Z=35$) nuclei because the number of virtual photons per unit energy interval, dN/dE_γ, is proportional to Z_T^2 (see Sec. I). The ^{12}C, ^{14}N, and ^{16}O nuclei in the emulsion also contribute to σ_{em}, although to a much lesser extent.

The theoretical values of the partial production cross sections for the different modes of breakup have been calculated by considering that the photon spectra for different targets at a constant value of the beam energy (200 GeV/nucleon) do not change significantly in shape but only in intensity. This means that the relative probabilities for the different modes of breakup in ED should be independent of the target, and the method of factorization may be used for the ED process. The calculated values of the partial production cross sections for different channels of the ED process, are included in Table II. In these calculations, the ED fragment factors, ϵ_P^F, of Ref. 6 were used. The total cross section for ED as well as the partial cross sections for different channels of breakup are comparable to the experimental ones.

D. P_t distribution of protons in the ^{31}Pp mode

Special attention was paid to the breakup mode ^{31}Pp, where the proton tracks were followed for at least 4 cm to ensure that these were not fast electron tracks in the very forward direction. In Fig. 3, we draw the P_t distribution of the protons emerging in the ^{31}Pp breakup mode. P_t were calculated from the measured values of the polar angles (θ) of protons, under the assumption that the projectile protons proceed in the forward direction with the same longitudinal momenta as that of the original ^{32}S ion. On the basis of the classical picture given in Ref. 3, the

TABLE II. Production cross section for the overall ED process and partial production cross sections in different modes of breakup.

Breakup mode	No. of events observed	Cross section in mb Experiment	Theory[b]
Overall ED process	197	511 ± 29[a]	345
^{31}Pp	72	121 ± 14	183
SiHe	25	42 ± 8	91
Si2p	26	44 ± 9	
AlHep	10	17 ± 5	21
Al3p	10	17 ± 5	
MgHe2p	13	22 ± 6	19
Mg2He	1	2 ± 2	
Mg4p	2	3 ± 2	
MgBe	1	2 ± 2	
NaLi2p	2		
Na2Hep	1		
NaHe3p	1		
Ne3He	2		
Ne2He2p	2		
NeHe4p	1		
F3Hep	2		
F2He3p	3		
FHe5p	1		
OLiHe3p	1		
O2He4p	3		
OHe6p	1		
NBHe2p	1		
NLi2He2p	1		
N3He3p	2		
N2He5p	1		
C3He4p	1		
BLi3He2p	1		
B2He7p	1		
BeLi2He5p	1		
5He6p	2		

[a]Correction applied to include the missing ^{31}Sn, ^{30}S2n, etc., modes (see Sec. III C of text).
[b]References 5 and 6.

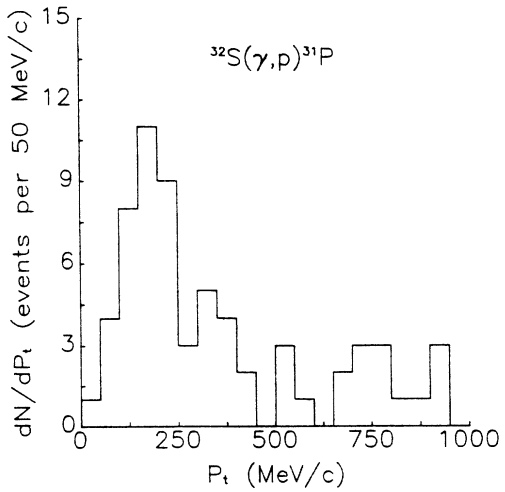

FIG. 3. Transverse momentum (P_t) distribution for protons in the breakup mode ^{31}Pp. P_t values were calculated from polar angles of protons produced in the ^{31}Pp mode.

momentum transferred due to the Coulomb collision is perpendicular to the motion of the projectile and is given by

$$P_t = \frac{2Z_P Z_T e^2}{bv} , \tag{3}$$

where eZ_P and eZ_T are the charges of the projectile and target, respectively, b is the impact parameter which is larger than the nuclear interaction radius and $v \simeq c$ is the velocity of the projectile nucleus. The impact parameter b is given by

$$b = 1.35(A_P^{1/3} + A_T^{1/3}) \text{ fm} , \tag{4}$$

where A_P and A_T are the projectile and target mass numbers, respectively. Using Eq. (3), the transverse momentum transferred to the ^{32}S nucleus from the AgBr targets is obtained as $P_t = 190$ MeV/c. Indeed, the peak in the P_t distribution shown in Fig. 3 is around 200 MeV/c. The momentum due to the decay of a resonant state according to $A \rightarrow B + C$ is given by $P_t = \sqrt{2m_0 \Delta E}$, where ΔE is the decay energy and m_0 is the reduced mass of $B + C$. This value of P_t corresponds to the decay energy ($\Delta E \simeq 21$ MeV) of an excited resonance state above the threshold value for the emission of a nucleon in the reaction $A \rightarrow B + C$. It is well known that for nuclei having mass above ~ 130 the giant dipole resonance is located at approximately[2]

$$E_{\text{GR}}^{(1)} = 80/A_P^{1/3} \text{ MeV} . \tag{5}$$

For lighter nuclei, however, the resonance energy falls off steadily[15] from the systematic value given by Eq. (5). For ^{32}S induced ED's, $E_{\text{GR}}^{(1)} \approx 25$ MeV. Wyckoff *et al.*[16] have studied the total photonuclear cross section $\sigma(\gamma,\text{tot})$ as a function of photon energy for a ^{32}S target. The giant dipole resonance in their experiment occurred in the range $18 < E < 23$ MeV. In view of the preceding arguments, the majority of the events in the ^{31}Pp breakup mode of this experiment may therefore be attributed to the absorption of giant dipole resonances. We were unable to perform the same analysis with other prominent modes on account of the low statistics. Some of the events such as C3He4p. B2He7p, BeLi2He5p. 5He6p, etc., may have been produced by the absorption of more than one photon or by the absorption of a single high-energy photon.

E. Multiplicity distributions of the He fragments in ED

Multiplicity distributions of the produced particles $P(n)$, have been studied extensively in hadron-hadron, hadron-nucleus, and nucleus-nucleus interactions in the past, since such studies are useful in understanding the production processes involved. As predicted by Koba, Nielsen, and Olesen,[17] $P(n)$ in high-energy hadron-hadron collisions obey a scaling law (KNO scaling), with an energy-independent function ψ. In a recent paper[18] it was observed that $P(n)$ for projectile He fragments also scales in nuclear interactions at ultrahigh energies. It is not our objective in this paper to see if $P(n)$ scales for the alpha fragments produced in electromagnetic dissociations. However, it is instructive to explore the nature of this distribution for alpha particles produced in ED's and to see if there is any significant departure of its behavior from nuclear collisions. In Fig. 4, we plot $P(n_\alpha)$ as a function of the scaled variable, $n_\alpha/\langle n_\alpha \rangle$ for alpha fragments, where n_α refers to the number of alpha particles produced in an interaction and $\langle n_\alpha \rangle$ is the average alpha multiplicity. The data points, in this figure, for the ED's are represented by "pluses." For comparison, the corresponding data points of alpha fragments from nuclear events are shown by full circles. In Ref. 18, it was observed that $P(n_\alpha)$ for alpha fragments emerging from nuclear events scale, i.e., the data points corresponding to various projectiles at different incident energies in the range 2–200 GeV/nucleon, lie on the same universal curve, shown in Fig. 4 by a dashed curve. It is interesting to note that the shapes of the multiplicity distributions for alpha fragments corresponding to nuclear and ED events are similar although the absolute values for the two are different. This difference may be a consequence of a different production mechanism.

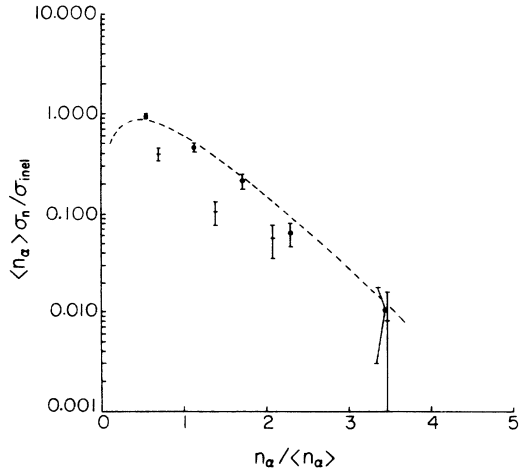

FIG. 4. Plot of $\langle n_\alpha \rangle P(n_\alpha)$ as a function of the scaled variable $n_\alpha/\langle n_\alpha \rangle$ for ED (+) and peripheral (●) events.

IV. CONCLUSIONS

The electromagnetic dissociation of the ^{32}S projectile at 200 GeV/nucleon represents 15% of the total number of events produced by ^{32}S in emulsion. For the same projectile (viz., ^{16}O), the production cross section of ED events has increased with projectile energy from 60 to 200 GeV/nucleon. This observation was also reported by Ardito *et al.*[7] At the same incident energy per nucleon (viz., 200 GeV/nucleon), the production cross section has also increased when the projectile charge is doubled from $Z=8$ to $Z=16$. The majority of events in the reaction $^{32}S(\gamma,p)^{31}P$ can be explained by the absorption of giant dipole resonances (Sec. III D).

The production cross sections for ED and the partial cross sections for different modes of breakup of ^{32}S have been determined experimentally and theoretically. These are found to be comparable with each other (Table II).

The multiplicity distribution, expressed in the normalized form, in ED's and nuclear events exhibit similar shapes. The fact that the two distributions do not overlap may be consequence of the different production mechanism of emerging alpha PF's in ED's (Sec. III E).

ACKNOWLEDGMENTS

We are thankful to Prof. G. Vanderhaeghe, the CERN technical staff, and the emulsion operating group for their help in the exposure and development of our emulsion stack. We are also thankful to Dr. S. N. Kim for his partial help in scanning. This work was supported by the National Science Foundation under Grant No. NSF/PHY8614797.

[1]D. L. Olson, B. L. Berman, D. E. Greiner, H. H. Heckman, P. J. Lindstrom, G. D. Westfall, and H. J. Crawford, Phys. Rev. C **24**, 1529 (1981).

[2]C. A. Bertulani and B. Baur, Phys. Rep. **163**, 299 (1988).

[3]J. D. Jackson, *Classical Electrodynamics,* 2nd ed. (Wiley, New York, 1975), p. 619.

[4]P. B. Price, R. Guoxiao, and W. T. Williams, Phys. Rev. Lett. **61**, 2193 (1988); J. C. Hill *et al.*, *ibid.* **60**, 999 (1988).

[5]C. Brechtmann and W. Heinrich, Z. Phys. A **330**, 675 (1988).

[6]C. Brechtmann and W. Heinrich, Z. Phys. A **331**, 463 (1988).

[7]N. Ardito *et al.*, Europhys. Lett. **6**, 131 (1988).

[8]K. Rybicki, Nuovo Cimento **49**, 203 (1967).

[9]A. Z. M. Ismail, M. S. El-Nagdy, K. L. Gomber, M. M. Aggarwal, and P. J. Jain, Phys. Rev. Lett. **52**, 1280 (1984); P. L. Jain, M. M. Aggarwal, and K. L. Gomber, Phys. Rev. C **34**, 726 (1986).

[10]M. I. Adamovich *et al.*, Phys. Rev. Lett. **62**, 2801 (1989); M. I. Adamovich *et al.*, Phys. Lett. **227**, 285 (1989).

[11]P. L. Jain and N. J. Wixon, Phys. Rev. Lett. **23**, 715 (1969); P. L. Jain, N. J. Wixon, D. A. Phillips, and J. T. Fecteau, Phys. Rev. D **1**, 813 (1970); N. J. Wixon, Ph.D. thesis, SUNY at Buffalo, 1970.

[12]K. Sengupta, G. Singh, T. Ritter, and P. L. Jain, Europhys. Lett. **8**, 15 (1988); and unpublished data of our laboratory.

[13]W. H. Barkas, *Nuclear Research Emulsions* (Academic, New York, 1963).

[14]G. D. Westfall, L. W. Wilson, P. J. Lindstrom, H. J. Crawford, D. E. Greiner, and H. H. Heckman, Phys. Rev. C **19**, 1309 (1979).

[15]F. E. Bertrand, Nucl. Phys. **A354**, 129c (1981).

[16]J. M. Wyckoff, B. Ziegler, H. W. Koch, and R. Uhlig, Phys. Rev. B **137**, 576 (1965); see also R. Alarcon, A. M. Nathan, S. F. LeBrun, and S. D. Hoblit, Phys. Rev. C **39**, 324 (1989).

[17]Z. Koba, H. B. Nielsen, and P. Olesen, Nucl. Phys. **B40**, 317 (1972).

[18]K. Sengupta, G. Singh, and P. L. Jain, Phys. Lett. B **222**, 301 (1989).